Optimal Resilient Power Grid Operation during the Course of a Progressing Wildfire

Salman Mohagheghi[a,*], Steffen Rebennack[b]

[a] *Electrical Engineering and Computer Science Department, Colorado School of Mines, Golden, CO 80401, USA*
[b] *Division of Economics and Business, Colorado School of Mines, Golden, CO 80401, USA*

Abstract

We study a two-stage stochastic and nonlinear optimization model for operating a power grid exposed to a natural disaster. Although this approach can be generalized to any natural hazard of continuous (and not instantaneous) nature, our focus is on wildfires. We assume that an approaching wildfire impacts the power grid by reducing the transmission capacity of its overhead lines. At the time when proactive decisions have to be taken, the severity of the wildfire is not known. This introduces uncertainty. In this paper, we extend previous work by more realistically capturing this uncertainty and by strengthening the mathematical programming formulation through standard reformulation techniques. With these reformulation techniques, the resulting two-stage, convex mixed-integer quadratically constrained programming formulation can be efficiently solved using commercial quadratic programming solvers as demonstrated on a case study on a modified version of the IEEE 123-bus test system with 100 scenarios. We also quantify the uncertainties through a second case study using the following three standard metrics of two-stage stochastic optimization: the expected value of perfect information, the expected result of using the expected value solution and the value of the stochastic solution.

Keywords: Convex reformulation, demand response, distributed energy

*Corresponding author
Email addresses: smohaghe@mines.edu (Salman Mohagheghi), srebenna@mines.edu (Steffen Rebennack)
URL: www.rebennack.net (Steffen Rebennack)

resources, Microgrid, mixed-integer quadratically constrained programming (MIQCP), natural disasters, SCENRED2, two-stage stochastic optimization

---

0. Notation

Wilfire Modeling

The values provided in this section represent the numbers used in the two case studies.

Conductor parameters:

d_c	conductor diameter; $1.83{\cdot}10^{-2}$ [m]
h_c	conductor height from the ground; 6 [m]
$I_{c,\max}$	conductor rating; 530 [A]
R_c	conductor resistance; $1.9{\cdot}10^{-4}$ [Ω/m]
$T_{c,\max}$	maximum permissible conductor surface temperature; 373 [°K]
ϵ_c	conductor emissivity; 0.5 [-]
μ_c	conductor absorption coefficient; 0.5 [-]

Fire parameters and variables:

L_f	fire flame length; 9 [m]
r_f	distance of fire to the object of interest; [m]
$r_f(0)$	initial distance of fire to the object of interest; 40 [m]
T_f	flame zone temperature; 1200 [°K]
v_f	fire rate of spread; [m/s]
W_f	fire flame width; 15 [m]
γ_f	fire flame tilt angle; 45 [degrees]
ϵ_f	fire flame zone emissivity; 0.5 [-]
ρ_f	fuel bulk density; 40 [kg/m^3]

Atmospheric and weather parameters and variables:

T_α ambient air temperature; 298 [°K]

v_w wind speed; [m/s]

Φ_s solar irradiance; 1000 [W/m^2]

λ_α atmospheric thermal conductivity; 0.0289 [W/m.°K]

μ_α dynamic viscosity of air; $2.01{\cdot}10^{-5}$[Pa.s]

θ_w wind direction with respect to the conductor normal; [degrees]

ρ_α air density; 1.0 [kg/m^3]

σ Stefan-Boltzman constant; $5.67{\cdot}10^{-8}$ [W/m^{2}K^4]

τ_α atmospheric transmissivity; 1.0 [-]

Heat flow variables:

Q_c convective heat loss rate per unit length of conductor; [W/m]

Q_r radiative heat loss rate per unit length of conductor; [W/m]

$Q_{r,f}$ radiative heat gain rate per unit length of conductor due to wildfire; [W/m]

Q_s solar radiant heat gain rate per unit length of conductor; [W/m]

Mathematical Programming Problem

Function:

$\mathbb{I}_{\mathcal{A}}(a)$ indicator function: 1 if $a \in \mathcal{A}$, 0 o/w

Sets/indices:

$b \in \mathcal{B} = \{1, \ldots, B\}$	buses in the network
$r \in \mathcal{B}$	root node (location of substation)
$b \in \mathcal{B}_m \subset \mathcal{B}$	buses in microgrid m
$b, j \in \mathcal{J}_m \subseteq \mathcal{B}_m$	DG at bus j in Microgrid m
$b, k \in \mathcal{K}_m \subseteq \mathcal{B}_m$	DR (controllable) load at bus k for Microgrid m
$b, l \in \mathcal{L} \subseteq \mathcal{B}$	load buses

$m \in \mathcal{M} = \{1, \ldots, M\}$	Microgrid
$p \in \mathcal{P} = \{a, b, c\}$	phases
$p \in \mathcal{P}^{\mathrm{DG}}_{j,m} \subseteq \mathcal{P}$	phases served by DG at bus j in Microgrid m
$p \in \mathcal{P}^{\mathrm{DR}}_{k,m} \subseteq \mathcal{P}$	phases served by DR at bus k in Microgrid m
$q \in \mathcal{Q} \subset \mathcal{B} \times \mathcal{B}$	branches in the network
$s \in \mathcal{S} = \{1, \ldots, S\}$	wildfire scenarios
$t \in \mathcal{T} = \{1, \ldots, T\}$	periods, times or stages

Data/parameters (capital letters):

α_l	priority level of load bus; in [0,1]; [-]
$C^{\mathrm{DG,res}}_{j,m,t}$	reserve price for DG; [$/kWh]
$C^{\mathrm{DR,res}}_{k,m,t}$	reserve price for DR; [$/kWh]
$C^{\mathrm{DG,gen}}_{j,m,t}$	generation cost for DG; [$/kWh]
$C^{\mathrm{DR,gen}}_{k,m,t}$	generation cost for DR (DR provides virtual generation through demand reduction); [$/kWh]
C^{sub}_{t}	generation cost for distribution substation; [$/kWh]
$C^{\mathrm{LR}}_{m,t}$	lost revenue due to load shedding; [$/kWh]
$H^{\mathrm{DR}}_{k,m,p,t}$	conversion factor to connect active and reactive generation for DR; [-]
M^{d}	penalty for demand shedding; [$/kWh]
$P_{l,p,t}$	active demand per load bus; [kW]
P_s	probability of scenario; [-]
$\overline{P}^{\mathrm{sub}}$	upper bound on substation generation; [kW]
$\overline{P}^{\mathrm{DG,gen}}_{j,m}$	upper bound on DG generation; [kW]
$\overline{P}^{\mathrm{DR,gen}}_{j,m,p,t}$	upper bound on DR virtual generation; [kW]
$Q_{l,p,t}$	reactive demand per load bus; [kVar]
$\overline{Q}^{\mathrm{sub}}$	upper bound on substation reactive generation; [kVar]
$\overline{Q}_{j,m}$	upper bound on reactive generation of DG; [kVar]
$\overline{S}_{q,s,t}$	line capacity; [kVA]

Further, we derive the total active demand per load bus

$$P_{l,t} := \sum\nolimits_{p\in\mathcal{P}} P_{l,p,t},$$

and the total active demand per Microgrid

$$P_{m,t} := \sum\nolimits_{l\in\mathcal{B}_m\cap\mathcal{L}} P_{l,t}.$$

Decision variables (small letters):

$f^{\mathrm{P}}_{p,q,s,t}$	active flow at branch q; [kW]; *free*
$f^{\mathrm{Q}}_{p,q,s,t}$	reactive flow at branch q; [kVar]; *free*
$p^{\mathrm{DG,res}}_{j,m,t}$	reserve quantity for DG; cumulative over all phases; [kWh]; *non-negative*
$p^{\mathrm{DR,res}}_{k,m,p,t}$	reserve quantity for DR; [kWh]; *non-positive*
$p^{\mathrm{DG,gen}}_{j,m,s,t}$	generation for DG; three-phase units will have the same generation for all phases; [kWh]; *non-negative*
$p^{\mathrm{DR,gen}}_{k,m,p,s,t}$	active generation for DR (virtual generation through active power demand reduction); [kWh]; *non-positive*
$p^{\mathrm{sub}}_{p,s,t}$	active generation of substation; [kWh]; *non-negative*
$p^{\mathrm{DG,gen,lin}}_{j,m,s,t}$	auxiliary variable, see (27); [kWh]; *non-negative*
$p^{\mathrm{DR,gen,lin}}_{k,m,s,t}$	auxiliary variable, see (31); [kWh]; *non-negative*
$q^{\mathrm{DG,gen}}_{j,m,s,t}$	reactive generation; three-phase units will have the same generation for all phases; [kVarh]; *non-negative*
$q^{\mathrm{DR,gen}}_{k,m,p,s,t}$	reactive generation for DR (virtual generation through reactive power demand reduction); [kVarh]; *non-positive*
$q^{\mathrm{sub}}_{p,s,t}$	reactive generation of substation; [kVarh]; *non-negative*
$u_{m,s,t}$	0: islanding, 1: connected; [-]; *binary*
$v_{l,s,t}$	0: shed, 1: connected; [-]; *binary*
$w_{l,m,s,t}$	auxiliary variable, see (32); [-]; *binary*

Naturally, any two Microgrids do not share common buses. This implies that the Microgrid index m can be dropped whenever the double indices "j, m" and "k, m" are present.

1. Introduction

Wildfires may get out of control and approach city limits, affecting also the power grid. The increased heat may limit transmission capabilities. The reliable transmission of power during such a disaster event is of foremost importance and may require a proactive transmission schedule. For instance, reserve requirements may have to be increased or load need to be adjusted for demand responsive nodes. One may also have to activate additional generators at different parts of the grid or shed load, as a last resort. When preparing for such a disaster event, uncertainty in the wildfire spread and severity needs to be taken into account accordingly. A resilient power grid is one that is able to withstand such a major disruption with limited degradation and can recover within a narrow timeframe with constricted costs [1]. Power grid resilience can be achieved in different ways based on the ultimate objective and the timeline of interest.

One way to achieve resilience is to use energy resources in addition to the main distribution substation. Using distributed energy resources such as distributed generation (DG), energy storage systems (ESS) and demand responsive (DR) loads as virtual generation can help improve the robustness of the power grid against contingencies [2, 3]. At the same time, much effort has been made in the literature on ensuring that a power network is able to restore power to the outage areas following a large scale disturbance. This has often been addressed within the context of electric service restoration, and the problem has been solved either in a centralized fashion [4, 5, 6] or using a decentralized approach based on multi-agent theory [7, 8]. Finally, some researchers have adopted security-constrained optimal power flow (SCOPF) approaches [9] to strengthen the power grid against forecasted contingencies. The objective here is to dispatch the generation resources in the power grid in such a way that all operational constrained are maintained not only for the normal operating condition, but for all credible contingencies. More recent SCOPF approaches have incorporated the probabilities and severities of the contingencies into account, thus making them stochastic and risk-based in nature [10]. While the literature

stands fairly comprehensive when it comes to preparing the grid for a natural disaster prior to the onset of the event (*i.e.*, through SCOPF approaches) or after it has run its course (*i.e.*, through electric service restoration), the management and dispatch of the power grid during the course of an event remains to be appropriately addressed. This is the intended focus of this paper.

In this paper, we study such a proactive system dispatch during a natural disaster. The mathematical programming model investigated is based on the two-stage stochastic optimization model proposed by Ansari and Mohagheghi, [11]. The disaster is modeled as a decrease in transmission capacity (at a single line). The two-stage nature of the optimization problem comes from the fact that proactive decisions, *i.e.*, distributed generation (DG) and demand response (DR) reserves, have to be taken before the impact on a certain transmission line is known. After the reduced capacity of that transmission line is observed, then the loads need to be served with the available transmission and generation capacities, given the reserves purchased; load shedding may be required or microgirs may be islanded. These are the second-stage decisions.

The focus of this paper lies in the improvement in modeling of the stochastic aspect of the wildfire, its impact on the capacity of the overhead lines, and the thorough treatment of the mathematical programming problem from an optimization perspective. Specifically, this paper has the following unique contributions:

- Systematic generation of scenarios for the two-stage stochastic optimization model and their optimal reduction to yield a tractable mathematical programming problem.
- Reformulation of the two-stage, nonlinear optimization problem to a two-stage, quadratic optimization problem. This yields in superior computational performance.
- Quantification of uncertainty and discussion of the optimal strategies through two case studies.

We continue in 2 by presenting our methodology to characterize the distribution of the stochastic line capacity as a result of an approaching wildfire. Next, we present the mathematical programming formulation in Section 3, while we discuss techniques to simplify its structure for better computational tractability in Sections 4. Section 5 contains two case studies. We conclude with Section 6 and we provide data for the case study in Appendix A.

2. Wildfire

2.1. Line Rating Fundamentals

A wildfire is an unplanned or unwanted natural or person-caused fire occurring in a natural setting [12]. It can affect any power grid component exposed to it. The damages can be either through direct contact (wooden poles, substations, or generators catching fire) or indirectly by increasing the temperatures beyond levels for which the equipment are designed. One type of power grid component which is in particular sensitive to wildfires is the overhead line. Excess heat released due to the wildfire can dramatically increase the surface temperature of the conductor, which in turn results in conductor sag. Temporary sag of the conductor reduces its distance to ground and increases the chances of flashover. At the same time, most conductors have a threshold beyond which excess elongation leads to permanent annealing of the steel core [13]. Any overhead line conductor has a maximum operating temperature that should not be surpassed. This is a design parameter that is provided by the manufacturer and depends on the size of the conductor, number of strands, height and spacing of towers, and the type of environment it is used at, among others. Maximum temperature determines the rating of the line [14, 15]:

$$I_{\max} = \sqrt{\frac{Q_c + Q_r - Q_s}{R_c(T_{c,\max})}}. \tag{1}$$

A wildfire progressing towards an overhead line can increase the conductor's surface temperature by transferring heat to the conductor through radiation and maybe convection. To counteract this, the rating of the line needs to be

dynamically adjusted so as to not exceed the maximum permissible temperature $T_{c,\max}$. This has been modeled in this paper as:

$$I_{\max} = \sqrt{\frac{Q_c + Q_r - Q_s - Q_{c,f} - Q_{r,f}}{R_c(T_{c,\max})}}. \tag{2}$$

2.2. Modeling Wildfire Impact on Line Rating

According to [14], the solar, radiative and convective heat loss/gain rates (without wildfire) can be estimated from the following equations. For the convective portion, forced heat loss in the presence of wind stream blowing at speed v_w and at an angle θ_w has been considered.

$$\begin{aligned} Q_c &= 0.0119 \cdot \left(\frac{d_c \cdot 1000 \cdot \rho_a v_w}{\mu_\alpha} \right) \cdot \lambda_\alpha \cdot K_{\text{angle}} \cdot (T_c - T_\alpha) && (3) \\ K_{\text{angle}} &= 1.194 - \sin(\theta_w) - 0.194\cos(2\theta_w) + 0.368\sin(2\theta_w) && (4) \\ Q_r &= \sigma \cdot \epsilon_c \pi \cdot d_c (T_c^4 - T_\alpha^4) && (5) \\ Q_s &= \mu_c \Phi_s d_c. && (6) \end{aligned}$$

The heat from the wildfire is mostly transferred through radiation. However, in some cases, heat transfer through convection is also possible. In our model, the convective heat transfer due to wildfire has been ignored, since it has been shown that this component exists only when the fire reaches the tower and is directly under the overhead line [16]. During this time, it is very likely that the line has been taken out of service by the utility operators as a precautionary measure to avoid the risk of flashover. This would therefore require a new dispatch of the power grid subject to network reconfiguration constraints that falls outside the scope of the current paper.

To accurately calculate radiative heat transfer from wildfire, the solid flame model proposed in [17] has been adopted. In this model, visible flame is considered to be a geometrical body that emits radiative heat uniformly throughout its entire surface area. According to this model, for a planar fire that moves towards target O located at height h_c above the ground and distance r_f from the fire, the radiative heat flux received by the target can be calculated as:

$$Q_{r,f} = \tau_\alpha \cdot \epsilon_f \sigma \cdot T_f^4 \big(\alpha_{vf}(r_{\inf}, \beta_{\inf}) + \alpha_{vf}(r_{\sup}, \beta_{\sup}) \big) \tag{7}$$

where:

$$r_{\text{inf}} = r_f \tag{8}$$

$$\beta_{\text{inf}} = \tan^{-1}\left(\frac{h_c}{r_{\text{inf}} - h_c \tan(\gamma_f)}\right) \tag{9}$$

$$r_{\text{sup}} = r_f - h_c \tan(\gamma_f) \tag{10}$$

$$\beta_{\text{sup}} = \tan^{-1}\left(\frac{h_c}{r_{\text{sup}} - \left(L_f - h_c \tan(\gamma_f)\right)}\right) \tag{11}$$

Function α_{vf} represents the view factor between the fire and the object of interest, and is a function of the fire width and tilt angle, as well as the distance from the fire flame zone to the object. This equation is provided in [17] and will not be repeated here for brevity.

The rate of spread of the fire front depends on the wind speed as well as the fuel bulk density [16]:

$$v_f = \frac{0.07(1 + v_w)}{\rho_f}. \tag{12}$$

This means that the distance of wildfire to the object of interest, *i.e.*, overhead line, at time t would be:

$$r_f(t) = r_f(0) - v_f \cdot t. \tag{13}$$

3. Mathematical Programming Problem Formulation

The goal of the optimization framework by Ansari and Mohagheghi [11] is to find a dispatch of energy resources, which allows for the optimal operation of the power grid during the course of a wildfire event. The optimization model has to balance DG and DR cost with the economic losses of islanding of a Microgrid and the penalty for load shedding. The amount of power available in each Microgrid is assumed to be bound by the reserves purchased beforehand. We follow this idea.

Just like in [11], the operator can take one or more of the following actions during emergency conditions in order to reduce the total load on its network:

(a) increase generation of autonomous DG units (given that sufficient generation capacity has been reserved beforehand),

(b) curtail the demand of DR loads (given that sufficient DR capacity has been reserved beforehand),

(c) island Microgrid completely, or

(d) shed loads as the last resort.

Each of the four actions above imply different type of costs.

We model our optimal resilient power grid operation problem during wildfires as a two-stage, mixed-integer nonlinear programming (MINLP) problem. The first stage decision variables are the power reserves purchased by the utility, *i.e.*, $p^{\mathrm{DG,res}}_{j,m,t}$ and $p^{\mathrm{DR,res}}_{k,m,p,t}$. The second stage (recourse) decision variables are the setpoints/dispatch commands for DG units, DR loads, islanding of Microgrids, and load shedding, for each scenario. The model reads as follows with the convention that small letters denote decision variables while capital letters are input data:

(Objective function)

$$
\begin{aligned}
\min \sum_{t\in\mathcal{T}}\Bigg(& \sum_{m\in\mathcal{M}}\sum_{j\in\mathcal{J}_m} C^{\mathrm{DG,res}}_{j,m,t}\cdot p^{\mathrm{DG,res}}_{j,m,t} \\
& - \sum_{m\in\mathcal{M}}\sum_{k\in\mathcal{K}_m}\sum_{p\in\mathcal{P}^{\mathrm{DR}}_{k,m}} C^{\mathrm{DR,res}}_{k,m,t}\cdot p^{\mathrm{DR,res}}_{k,m,p,t} \\
& + \sum_{s\in\mathcal{S}} P_s\cdot\Big(C^{\mathrm{sub}}_t \sum_{p\in\mathcal{P}} p^{\mathrm{sub}}_{p,s,t} \\
& + \sum_{m\in\mathcal{M}} u_{m,s,t}\sum_{j\in\mathcal{J}_m} C^{\mathrm{DG,gen}}_{j,m,t}\sum_{p\in\mathcal{P}^{\mathrm{DG}}_{j,m}} p^{\mathrm{DG,gen}}_{j,m,s,t} \\
& - \sum_{m\in\mathcal{M}} u_{m,s,t}\sum_{k\in\mathcal{K}_m} C^{\mathrm{DR,gen}}_{k,m,t}\sum_{p\in\mathcal{P}^{\mathrm{DR}}_{k,m}} p^{\mathrm{DR,gen}}_{k,m,p,s,t} \\
& + \sum_{m\in\mathcal{M}} C^{\mathrm{LR}}_{m,t}\cdot P_{m,t}\cdot(1-u_{m,s,t}) \\
& + M^{\mathrm{d}} \sum_{l\in\mathcal{L}\setminus\cup_{m\in\mathcal{M}}\mathcal{B}_m} \alpha_l\cdot(1-v_{l,s,t})\cdot P_{l,t} \\
& + M^{\mathrm{d}} \sum_{m\in\mathcal{M}}\sum_{l\in\mathcal{L}\cap\mathcal{B}_m} \alpha_l\cdot(1-v_{l,s,t})\cdot u_{m,s,t}\cdot P_{l,t}\Big)\Bigg)
\end{aligned}
\tag{14}
$$

(Power outflow of substation, $\forall p \in \mathcal{P},\ s \in \mathcal{S},\ t \in \mathcal{T}$)

$$\text{s.t. } p^{\text{sub}}_{p,s,t} = \sum_{q'=(r,\cdot)\in\mathcal{Q}} f^{\text{P}}_{p,q',s,t} \tag{15}$$

$$q^{\text{sub}}_{p,s,t} = \sum_{q'=(r,\cdot)\in\mathcal{Q}} f^{\text{Q}}_{p,q',s,t} \tag{16}$$

(Power flow at buses, $\forall b \in \mathcal{B},\ p \in \mathcal{P},\ s \in \mathcal{S},\ t \in \mathcal{T}$)

$$\begin{aligned}\text{s.t. } & \sum_{q=(\cdot,b)\in\mathcal{Q}} f^{\text{P}}_{p,q,s,t} + \sum_{m\in\mathcal{M}} \mathbb{I}_{\mathcal{J}_m}(b)\cdot\mathbb{I}_{\mathcal{P}^{\text{DG}}_{b,m}}(p)\cdot p^{\text{DG,gen}}_{b,m,s,t} = \\ & \sum_{q'=(b,\cdot)\in\mathcal{Q}} f^{\text{P}}_{p,q',s,t} + \mathbb{I}_{\mathcal{L}}(b)\cdot P_{b,p,t}\cdot v_{b,s,t} \\ & + \sum_{m\in\mathcal{M}} \mathbb{I}_{\mathcal{K}_m}(b)\cdot\mathbb{I}_{\mathcal{P}^{\text{DR}}_{b,m}}(p)\cdot p^{\text{DR,gen}}_{b,m,p,s,t}\cdot v_{b,s,t}\end{aligned} \tag{17}$$

$$\begin{aligned} & \sum_{q=(\cdot,b)\in\mathcal{Q}} f^{\text{Q}}_{p,q,s,t} + \sum_{m\in\mathcal{M}} \mathbb{I}_{\mathcal{J}_m}(b)\cdot\mathbb{I}_{\mathcal{P}^{\text{DG}}_{b,m}}(p)\cdot q^{\text{DG,gen}}_{b,m,s,t}\cdot u_{m,s,t} = \\ & \sum_{q'=(b,\cdot)\in\mathcal{Q}} f^{\text{Q}}_{p,q',s,t} + \mathbb{I}_{\mathcal{L}}(b)\cdot Q_{b,p,t}\cdot v_{b,s,t} \\ & + \sum_{m\in\mathcal{M}} \mathbb{I}_{\mathcal{K}_m}(b)\cdot\mathbb{I}_{\mathcal{P}^{\text{DR}}_{b,m}}(p)\cdot q^{\text{DR,gen}}_{b,m,p,s,t}\cdot v_{b,s,t}\end{aligned} \tag{18}$$

(Line flow, $\forall p \in \mathcal{P},\ q \in \mathcal{Q},\ s \in \mathcal{S},\ t \in \mathcal{T}$)

$$\text{s.t. } (f^{\text{P}}_{p,q,s,t})^2 + (f^{\text{Q}}_{p,q,s,t})^2 \le (\overline{S}_{q,s,t})^2 \tag{19}$$

(Islanding of Microgrids, $\forall m \in \mathcal{M},\ p \in \mathcal{P},\ s \in \mathcal{S},\ t \in \mathcal{T}$)

$$\begin{aligned}\text{s.t. } & (f^{\text{P}}_{p,q,s,t})^2 + (f^{\text{Q}}_{p,q,s,t})^2 \le (\overline{S}_{q,s,t})^2\cdot u_{m,s,t} \\ & \qquad \forall q \in \mathcal{Q},\ b \in \mathcal{B}_m \text{ with } q=(\cdot,b) \text{ or } q=(b,\cdot)\end{aligned} \tag{20}$$

(Variable bounds and variable relation,
$\forall m \in \mathcal{M},\ j \in \mathcal{J}_m,\ k \in \mathcal{K}_m,\ p \in \mathcal{P}^{\text{DR}}_{k,m},\ s \in \mathcal{S},\ t \in \mathcal{T}$)

$$\text{s.t. } 0 \leq \sum_{p \in \mathcal{P}^{\mathrm{DG}}_{j,m}} p^{\mathrm{DG,gen}}_{j,m,s,t} \leq p^{\mathrm{DG,res}}_{j,m,t} \leq \overline{P}^{\mathrm{DG,gen}}_{j,m} \tag{21}$$

$$-\overline{P}^{\mathrm{DR,gen}}_{k,m,p,t} \leq p^{\mathrm{DR,res}}_{k,m,p,t} \leq p^{\mathrm{DR,gen}}_{k,m,p,s,t} \leq 0 \tag{22}$$

$$0 \leq \sum_{p \in \mathcal{P}} p^{\mathrm{sub}}_{p,s,t} \leq \overline{P}^{\mathrm{sub}} \tag{23}$$

$$0 \leq \sum_{p \in \mathcal{P}^{\mathrm{DG}}_{j,m}} q^{\mathrm{DG,gen}}_{j,m,s,t} \leq \overline{Q}_{j,m} \tag{24}$$

$$q^{\mathrm{DR,gen}}_{k,m,p,s,t} = H^{\mathrm{DR}}_{k,m,p,t} p^{\mathrm{DR,gen}}_{k,m,p,s,t} \tag{25}$$

$$0 \leq \sum_{p \in \mathcal{P}} q^{\mathrm{sub}}_{p,s,t} \leq \overline{Q}^{\mathrm{sub}} \tag{26}$$

The objective function (14) minimizes the sum of the reservation cost of DG and DR, and the weighted cost of substation generation, DG generation, DR demand reduction, lost revenue for islanded Microgrids, as well as the load shedding penalties (which do not apply within an islanded Microgrid) based on the probability of each scenario. We model demand response as a negative load, implying that the corresponding decision variables $p^{\mathrm{DR,res}}_{k,m,p,t}$ and $p^{\mathrm{DR,gen}}_{k,m,p,s,t}$ are non-positive. In addition, in our calculations, we have ignored the cost of reactive power generation. This assumption has been made for simplicity, and does not affect the generality of the solution.

The (linear) power flow equations (15)-(18) constitute the main part of the constraints. Only flow of active and reactive power through the branches have been considered here, and node voltages have been ignored. It can be assumed that the node voltages are regulated using voltage regulating transformers along the feeders and the on-load tap changer at the substation transformer. The active and reactive generation by the substation is distributed among the connected branches, (15)-(16). The notation $(b, \cdot) \in \mathcal{Q}$ with $b \in \mathcal{B}$ means that we sum over all branches going out of bus b, while in case of $(\cdot, b)$ we sum over all branches coming into bus b. For each bus b, (17)-(18) balance incoming flow into b plus generation at b with outgoing flow out of b plus load at b plus DR load reductions at b. Active power load shedding implies that the demand

response is not available at the node, either. We assume that DG can only supply reactive power if the corresponding Microgrid is islanded, otherwise it would operate in a unity power factor mode if connected to the grid. We allow negative flow, indicating that power is transported "backwads" in the direction of the substation.

The line flow constraints (19) restrict the active and reactive power flow through each line. If a distribution line cannot serve a particular phase p, then the corresponding upper bound $\overline{S}_{p,q,s,t}$ is assigned value zero. If a Microgrid is islanded, the corresponding variable $u_{m,s,t}$ has value 0. Then, constraints (20) shut off any incoming and outgoing power flow from that Microgrid. The bounds on the decision variables are given in (21)-(26). Notice, (21) and (22) couple the reservation amount with the actual generation for both DG and DR.

We assume that the substation can produce different amounts for each phase, both active and reactive, while DG needs to serve the exact same quantity for each phase. Thus, we drop the phase index, p, for $p^{\mathrm{DG,gen}}_{k,m,s,t}$. In contrast, DR can have different levels per phase while for simplicity it has been assumed that the active and reactive generation are coupled in a way that power factor remains constant; see (25).

Note that there is a unique branch coming into any bus because of the radial network. However, multiple branches may go out of any bus. Further note that the binary decision variables $u_{m,s,t}$ and $v_{m,s,t}$ carry a scenario index. This challenges popular decomposition methods like the Benders decomposition (or integer L-shaped method). They are not readily applicable. Instead, specialized algorithms need to be applied, if desired.

In our two-stage stochastic programming model, we utilize a (linear) pipeline model for the power flow between buses. For our application, such a pipeline model is sufficient because it can assumed that the utility has enough voltage regulating transformers and shunt capacitors along the feeders to ensure that all node voltages are within acceptable bounds. Although not considered here, our model can be enhanced by adoption of full AC power flow equations. Such a model would introduce non-convexities into the mathematical programming

formulation, requiring different solution strategies [18, 19].

The presented model is a mixed-integer, quadratically constrained, quadratic mathematical programming problem (MIQCQP), because it contains both bilinear terms in the objective function and quadratic terms in the constraints.

4. Linearization: Convex MIQCP

We can use standard linearization techniques to transform the NLP formulation (14)-(26) into a convex, mixed-integer quadratically constrained programming (MIQCP) problem [20]. This allows the usage of the commercial solvers like CPLEX or GuRoBi, which are more robust and powerfull compared to global optimization solvers currently available.

Therefore, we linearize the objective function as follows. The bilinear terms, as product of binary and continuous variable,

$$p^{\mathrm{DG,gen,lin}}_{j,m,s,t} := u_{m,s,t} \sum_{p \in \mathcal{P}^{\mathrm{DG}}_{j,m}} p^{\mathrm{DG,gen}}_{j,m,s,t} \tag{27}$$

are linearized by the following set of linear constraints

$$p^{\mathrm{DG,gen,lin}}_{j,m,s,t} \leq u_{m,s,t} \sum_{p \in \mathcal{P}^{\mathrm{DG}}_{j,m}} \overline{P}^{\mathrm{DG,gen}}_{j,m} \tag{28}$$

$$p^{\mathrm{DG,gen,lin}}_{j,m,s,t} \leq \sum_{p \in \mathcal{P}^{\mathrm{DG}}_{j,m}} p^{\mathrm{DG,gen}}_{j,m,s,t} \tag{29}$$

$$p^{\mathrm{DG,gen,lin}}_{j,m,s,t} \geq p^{\mathrm{DG,gen}}_{j,m,s,t} - (1 - u_{m,s,t}) \sum_{p \in \mathcal{P}^{\mathrm{DG}}_{j,m}} \overline{P}^{\mathrm{DG,gen}}_{j,m}, \tag{30}$$

for all $j \in \mathcal{J}_m,\ m \in \mathcal{M},\ s \in \mathcal{S},\ t \in \mathcal{T}$. This way, we obtain one decision variable over all phases instead of $|\mathcal{P}^{\mathrm{DG}}_{j,m}|$ decision variables, one for each phase. It is important to notice that (28)-(30) are equivalent to (27). We treat the other term

$$p^{\mathrm{DR,gen,lin}}_{k,m,s,t} := u_{m,s,t} \sum_{p \in \mathcal{P}^{\mathrm{DR}}_{k,m}} p^{\mathrm{DR,gen}}_{k,m,s,t} \tag{31}$$

in a similar way, while respecting its non-positivity.

The product of two binary variables

$$w_{l,m,s,t} := (1 - v_{l,s,t}) \cdot u_{m,s,t} \tag{32}$$

is a binary variable itself, expressed via

$$w_{l,m,s,t} \leq 1 - v_{l,s,t} \tag{33}$$

$$w_{l,m,s,t} \leq u_{m,s,t} \tag{34}$$

$$w_{l,m,s,t} \geq u_{m,s,t} - v_{l,s,t}, \tag{35}$$

for all $m \in \mathcal{M},\ l \in \mathcal{L} \cap \mathcal{B}_m,\ s \in \mathcal{S},\ t \in \mathcal{T}$.

The linearization for constraints (17) is trivial: remove the variable $v_{b,s,t}$ and add the following constraints

$$p^{\mathrm{DR,gen}}_{k,m,s,t} \geq -\overline{P}^{\mathrm{DR,gen}}_{k,m,t} v_{k,s,t} \tag{36}$$

for all $k \in \mathcal{K}_m,\ m \in \mathcal{M},\ s \in \mathcal{S},\ t \in \mathcal{T}$. We apply a similar reformulation to the bilinear terms in constraints (18). Because active and reactive DR is coupled via (25), we eliminate the decision variables $q^{\mathrm{DR,gen}}_{k,m,p,s,t}$ from the model.

The line flow constraints (19) contain quadratic terms of continuous variables. There is no exact linearization of these nonlinear terms. However, the resulting constraints yield a convex set. The same holds true for islanding constraints (20), for any binary value of $u_{m,s,t}$. Thus, there is no need for special treatment. Nevertheless, we can lower the computational burden by reformulating the islanding of Microgrids condition (20) to avoid quadratic constraints as follows

$$-\overline{S}_{q,s,t} \cdot u_{m,s,t} \leq f^{\mathrm{P}}_{p,q,s,t} \leq \overline{S}_{q,s,t} \cdot u_{m,s,t} \tag{37}$$

$$-\overline{S}_{q,s,t} \cdot u_{m,s,t} \leq f^{\mathrm{Q}}_{p,q,s,t} \leq \overline{S}_{q,s,t} \cdot u_{m,s,t} \tag{38}$$

for all $q \in \mathcal{Q},\ b \in \mathcal{B}_m$ with $q = (\cdot, b)$ or $q = (b, \cdot)$. For each quadratic constraint (20), we require four linear constraints (37)-(38). Though the reformulation (37)-(38) is equivalent to (20) for any binary value $u_{m,s,t}$, the corresponding RMIQP, *i.e.*, the relaxation (or replacement) of the binary restrictions by continuous variables in [0,1] of the MIQCP, of the reformulated problem is stronger for $u_{m,s,t} \in \left(0, \frac{1}{2}\right)$ and weaker for $u_{m,s,t} \in \left(\frac{1}{2}, 1\right)$.

A convex MIQCP solver, like CPLEX, can solve the resulting, transformed problem to proven optimality, for suitable problem sizes.

5. Case Study

5.1. System Data

We use the same test system as in [11] which is a modified version of the IEEE 123-bus test distribution system [21] to feature four Microgrids, *cf.* Fig. 1. For each Microgrid, the locations and sizes of the DG units and DR loads are listed in Appendix A. The DG units in this paper have all been considered to be dispatchable as only these units would be applicable to the energy dispatch problem studied here. Non-dispatchable units such as wind turbines and solar PV, if present, can be modeled as stochastic negative load. From the standpoint of the problem formulation presented in this paper, this would only increase the number of stochastic scenarios, and would not change the structure of the problem. Linear cost structures have been assumed for both DG and DR resources. Cost data is taken from [22], and appears in Appendix A. The substation transformer is a 5MVA, 115kV:4.6kV delta-grounded Y three-phase transformer. A 336,400 26/7 ACSR conductor has been considered for the three-phase main feeders, with a capacity 530A, diameter 0.721 inches and a resistance of 0.306 Ω/mile. The loads in [21] have been increased by a factor of 50% in order to simulate a heavy loading condition.

In contrast to [11], we assume a time horizon of a single period, *i.e.*, $T = 1$. The reason is that the presented formulation (14)-(26) (as well as the formulation presented in [11]) decouples with the periods, t. With other words, there is no coupling of the stages. There are different real-world aspects which may need to be incorporated into the model and which introduce such a time-coupling; for instance, fuel limitations for the generators.

5.2. Random Sampling for Line Capacity

It is assumed here that wildfire parameters and fuel data are given (see Sect. 0). However, wind speed and direction, which can affect conductor cooling as

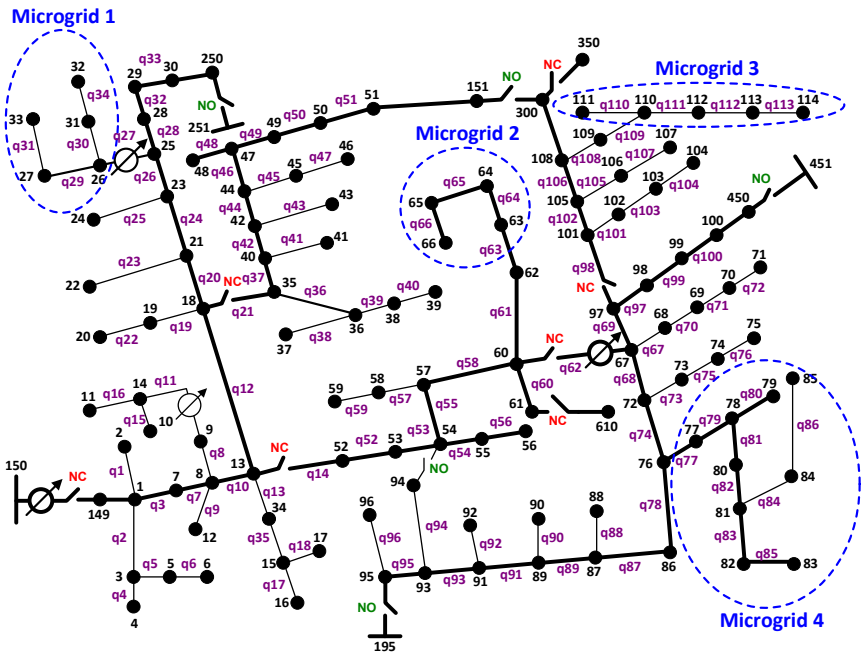

Figure 1: Schematic diagram of the test system with the added Microgrids. Picture adopted and redrawn from [11].

well as heat gained from the wildfire, are assumed uncertain. In this paper, wind speed is modeled by a Weibull distribution function with scale and shape factors 1.5 and 2.0, respectively. This represents a site where wind blows fairly consistent, but there are periods where winds blow harder than typical speeds [23]. On the other hand, a Von Mises probability distribution function has been assumed for wind direction, as it can accurately reflect the angles by which wind blows towards the conductor [23]. A mean of zero and a k-factor of 8 have been assumed for the distribution to model directions from -90° to +90° with respect to the axis normal to the conductor. Wind speed and direction are considered to be uncorrelated in this paper, and random samples are taken from the two distribution functions and are paired together to create one sample for the stochastic problem. For each sample, convective, radiative and solar heat loss/gain factors are calculated from (3)-(6), which are then used to calculate

the normal (no fire) conductor capacity based on (1). The distance of wildfire from the object (overhead line) is then calculated from (12) and (13), and is used to estimate the radiative heat gain due to wildfire from (7)-(11). The conductor capacity is then updated based on (2). The ratio of conductor capacity with and without fire effects determines how much of the original conductor capacity is available under the current wildfire threat. This value is then used as a sample for line capacity $\overline{S}$.

In an effort to approximate the "true" distribution for the line capacities when a wildfire is approaching, we draw 10,000 independent samples, with the procedure described above and in Sect. 2. The resulting empirical (cumulative) distribution function is shown in Fig. 2, while Fig. 3 depicts the corresponding probability density function. Naturally, we assume that each sample has the same probability of occurrence.

In order to yield a computationally tractable mathematical programming problem while assuring a good approximation of the distribution imposed by the 10,000 samples drawn, we utilize scenario reduction. Specifically, we use the software SCENRED2 linked to GAMS [24]. In a nutshell, optimal scenario reduction seeks a (discrete) probability distribution, which is the best approximation of our distribution given by the 10,000 samples, whose support consists of a subset of these 10,000 samples, with respect to some appropriate distance measure. As we choose to reduce the number of scenarios to 100, this implies that SCENRED2 selects 100 samples out of the 10,000. By adjusting their individual probability, these 100 samples can closely approximate the original distribution. The new probabilities are calculated by SCENRED2 as well. Thus, these 100 samples no longer have the same probability.

5.3. Computational Results

We have implemented the two-stage stochastic programming models in the modeling language GAMS (version 24.1.2). The MILPs are solved using CPLEX (version 12.6.0.1). We execute our computations on a standard desktop computer running Intel(R) Core(TM) i7 CPU @ 2.93Ghz on a 64 bit Windows

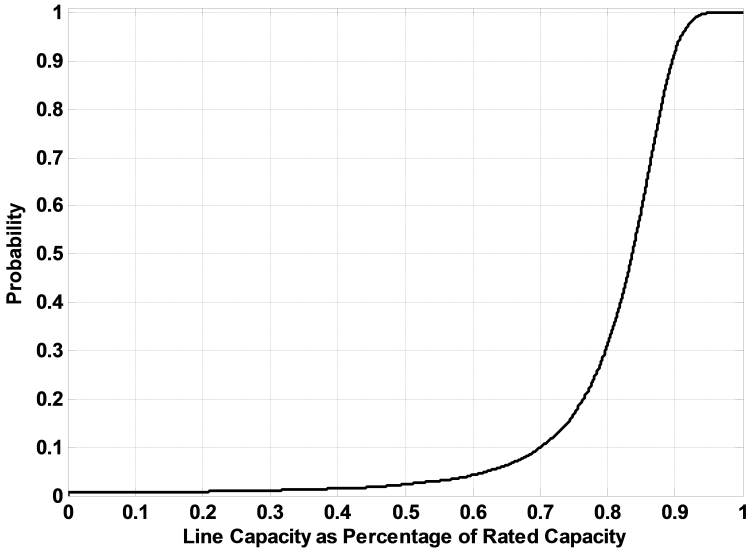

Figure 2: Empirical distribution function.

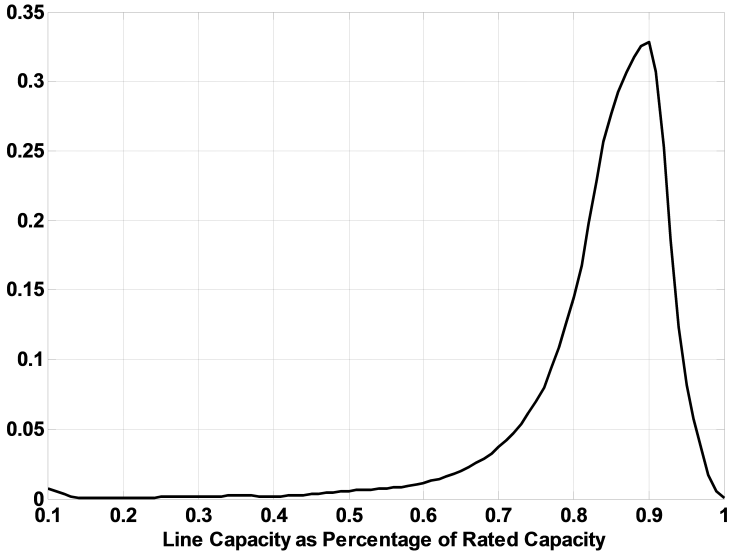

Figure 3: Approximated probability density function for the 10,000 sample points.

operating system with 12 GB Ram.

5.3.1. Case Study I: Wildfire Approaches Line $q12 = (13, 18)$

In our first case study, we mainly demonstrate the following two features of the proposed model:

1. The effects on the computational burden without the reformulation, as proposed in Sec. 4, and

2. The phase transition of the optimal solution, dependent on the choice of the load shedding penalty.

For the first point, consider Table 1. In this table, we summarize the computational results of all nonlinear solvers linked to GAMS which can solve the MIQCQP model as proposed in Sect. 3. Recall that this is a mixed-integer nonliner programming problem with quadratic objective function and quadratic constraints. We have used standard settings for all solvers and remark that the computational performance may be significantly enhanced by parameter tuning.

We have excluded GuRoBi, CPLEX, MOSEK and XPRESS as they do not support the solution of such a model, currently (the resulting RMIQCQP is non-convex). Also, we report the solution of BonminH as the commercially supported version of Bonmin. We have also excluded SBB as it encountered numerical stability problems.

We set the maximum running time to 12 hours and the relative optimality gap to 10^{-8}. The problem instance consists of 100 scenarios with a load shedding penalty of $M^d = 1,000$ [\$ / MWh]. The instance contains 79,922 decision variables of which are 8,900 are binary and 76,301 constraints. This is a very large-scale, global optimization problem.

We make several observations from Table 1. None of the global solvers was able to compute a proven optimal solution within 12 hours; none of the local solvers computed an optimal solution. Remarkable is the performance of ANTIGONE and GloMIQO which both computed an optimal solution and provided good lower bounds on the optimal solution; the best lower bound was

Solver	Best solution	CPU time best sol. found [hh:mm:ss]	Lower bound
AlphaECP, [25]	34,375.61	05:43:56	n/a
ANTIGONE, [26]	28,404.41	04:54:19	28,361.50
BARON, [27]	28,800.07	11:36:35	28,261.79
BonminH	883,250.00†‡	00:00:00†‡	n/a
COUENNE	883,250.00‡	00:00:00‡	27.724.52
DICOPT, [28]	34,375.61†	00:00:34†	n/a
GloMIQO, [29]	28,404.41	03:10:37	28,354.98
KNITRO, [30]	883,250.00‡	00:00:00‡	n/a
LINDO, [31]	883,250.00‡	00:00:00‡	n/a
LINDOGlobal, [31]	883,250.00‡	00:00:00‡	$-\infty$
SCIP, [32]	28,411.99	10:57:00	28,384.60

Table 1: Performance of various local and global solvers for the original MIQCQP formulation as presented in Sect. 3. The optimal objective function value is 28,404.41. †: solver terminated early within 1 hour; ‡: the starting point could not be improved

computed by SCIP. These three solvers clearly outperformed the other solvers for this problem instance.

Thus, the results in Table 1 dramatically demonstrated the need for a "good" problem formulation to ensure computational tractability. The key message is that the original MIQCQP cannot be solved within 12 hours while the reformulated convex MIQCPs solve within a few seconds.

Next, consider Table 2. It presents an optimal solution for different values of the load shedding penalty M^d for the equivalent convex MIQCP. Thus, the first instance of Table 2 corresponds to the instances of Table 1. We observe that the solution changes at a penalty of 25,000 $ per MWh. For the lower values, no DG and DR are utilized. Loads are shed for the scenarios for which the line capacity of branch (13,18) is reduced to the point that not all load can be served. In these cases, Microgrid 1 is islanded first. At a penalty 25,000

and above, DG and DR are activated. Thus, more loads can be served and the number of shedded buses drops.

Observe that the total number of load buses shed is not the same for the first five penalty factors. However, the total kWhs shed are the same. Thus, the different values reflect alternative optimal solutions. This is because our MIQCP model does not penalize the number of buses shed but, instead, the total kWhs shed are penalized. For instance, the load at buses 38 and 39 equals the load at bus 43. If the number of load buses shed should be minimized as well, then we suggest to solve another optimization problems as follows:

$$\min \sum_{m\in\mathcal{M}}\sum_{s\in\mathcal{S}}\sum_{t\in\mathcal{T}} u_{m,s,t} \tag{39}$$

$$\text{s.t. } z \leq \text{target cost} \tag{40}$$

$$(15) - (26), \tag{41}$$

where z represents the objective function value (14) and "target cost" are targeted total cost, *e.g.*, the optimal objective function value of the MIQCP solved.

5.3.2. Case Study II: Wildfire Approaches Line $q10 = (8, 13)$

With this case study, we

1. discuss the optimal solution values of the two-stage stochastic optimization model, and we

2. quantify the value of the stochastic solution and its approximation quality with respect to the 10,000 samples drawn.

Table 3 shows the results for the case of a wildfire approaching line (8,13). We have used 100 scenarios and a load shedding penalty, M^d, of 50,000 $ per MWh shed. The expected cost are $296,677.52. The solution has been computed in 465 seconds by CPLEX, within a relative tolerance of 10^{-8}.

Note that it is optimal to reserve the maximum quantity for DG. This is not true for DR. Out of the 100 scenarios, only 18 lead to load shedding (including islanding). These 18 scenarios occur with a probability of 3.37%. In contrast,

M^d	Optimal objective func. value	Number of load buses shed	1st stage cost		2nd stage cost						CPU time [seconds]
			DG reserve cost	DR reserve cost	Substation generation cost	Lost Revenue (MG)	Load shedding penalty	MG load shedding penalty	DG generation cost	DR cost	
1,000	28,404.41	180			24326.33	54.00	4,024.1				7.20
2,500	34,440.53	180			24326.33	54.00	10,060.2				7.87
5,000	44,500.73	178			24326.33	54.00	20,120.4				9.13
7,500	54,560.93	178			24326.33	54.00	30,180.6				23.68
10,000	64,621.13	178			24326.33	54.00	40,240.8				16.84
25,000	124,503.92	160	196.06	183.98	24328.55	36.24	97,302.5	2448.0	5.29	3.30	8.54
50,000	224,254.42	161	196.06	183.98	24328.55	36.24	194,605.0	4896.0	5.29	3.30	6.55
75,000	324,004.92	161	196.06	183.98	24328.55	36.24	291,907.5	7344.0	5.29	3.30	6.65
100,000	423,755.42	160	196.06	183.98	24328.55	36.24	389,210.0	9792.0	5.29	3.30	6.96

Table 2: Optimal solution for different load shedding penalties for a wildfire approaching branch between bus 13 and 18. The MIQCP was solved with CPLEX. No value indicates a value of zero.

when there is no DG and DR reserve, then the probability of a load shedding is 13.3%.

In general, the results as presented in Table 3 indicate that optimal values of DG and DR will be reserved based on the expected likelihood of different wildfire event scenarios. These reserves will then be dispatched during the course of the event. It is interesting to see that in some instances (*i.e.*, low threat event scenarios), the reserves are not fully used. This is natural because they are purchased with an eye on all possible event scenarios. It can be seen that for a high threat event scenario, all the reserves purchased are utilized.

In two-stage stochastic optimization, the paradigm is to make the first stage decision(s) before the uncertainty in the second stage unfolds, *i.e.*, we make our decision in a "here-and-now" fashion. In contrast, if one can wait until the uncertainty has unfolded, then we obtain a "wait-and-see" solution which serves as benchmark for the stochastic approach: the *expected value of perfect information* (EVPI) is the difference in the optimal objective function value between the "here-and-now" and the "wait-and-see" problems. The EVPI is the price we are willing to pay in order to gain perfect information.

When solving the two-stage stochastic MIQCP as a deterministic problem, naturally one chooses the expected value for the uncertain parameter, *i.e.*, the expected line capacity. The resulting optimal solution is called the *expected value* (EV) *solution*. For our problem instance, the EV solution yields zero DG and DR reserve, as the expected line capacity still allows to meet all load. This is true for the 10,000 sample case as well as for the reduced 100 samples. Thus, the optimal solution is to meet all demand via the substation, as long as the substation generation cost is less than DG/DR cost which is in turn less than the load shedding penalty. As long as this relation is met, the optimal solution does not change. When implementing the EV first stage solution and optimally adjusting the second stage decision variables for all scenarios, we obtain the *expected result of using the EV* ($\mathbb{E}$EV) *solution*. The *value of the stochastic solution* (VSS) is then the difference between the $\mathbb{E}$EV and the stochastic solution.

First stage variables				Line capacity	Low fire threat			Medium fire threat			Extreme fire threat		
					4.343			3.400			0.872		
	a	b	c		a	b	c	a	b	c	a	b	c
				p^{sub}	4.702	3.654	4.491	3.732	2.923	3.475	1.491	0.996	1.246
				q^{sub}	1.935	1.360	1.658	1.815	1.360	1.650	0.589	0.325	0.410
$p^{\text{DG,res}}_{31,1}$		0.20		$p^{\text{DG,gen}}_{31,1}$	–	–	0.000	–	–	0.000	–	–	0.200
$p^{\text{DG,res}}_{63,2}$		0.60		$p^{\text{DG,gen}}_{63,2}$	0.000	0.000	0.000	0.170	0.170	0.170	0.200	0.200	0.200
$p^{\text{DG,res}}_{65,2}$		0.90		$p^{\text{DG,gen}}_{65,2}$	0.000	0.000	0.000	0.270	0.270	0.270	0.300	0.300	0.300
$p^{\text{DG,res}}_{110,3}$		0.25		$p^{\text{DG,gen}}_{110,3}$	0.250	–	–	0.250	–	–	0.250	–	–
$p^{\text{DG,res}}_{78,4}$		0.90		$p^{\text{DG,gen}}_{78,4}$	0.000	0.000	0.010	0.300	0.300	0.300	0.300	0.300	0.300
$p^{\text{DR,res}}_{31,1}$	–	–	-0.064	$p^{\text{DR,gen}}_{31,1}$	–	–	-0.028	–	–	0.000	–	–	-0.064
$p^{\text{DR,res}}_{32,1}$	–	–	-0.064	$p^{\text{DR,gen}}_{32,1}$	–	–	-0.028	–	–	0.000	–	–	-0.064
$p^{\text{DR,res}}_{33,1}$	-0.080	–	–	$p^{\text{DR,gen}}_{33,1}$	-0.080	–	–	0.000	–	–	-0.080	–	–
$p^{\text{DR,res}}_{63,2}$	-0.080	–	–	$p^{\text{DR,gen}}_{63,2}$	-0.080	–	–	-0.080	–	–	-0.080	–	–
$p^{\text{DR,res}}_{65,2}$	-0.112	-0.104	-0.218	$p^{\text{DR,gen}}_{65,2}$	-0.112	0.000	0.000	-0.112	0.000	-0.120	-0.100	0.104	-0.120
$p^{\text{DR,res}}_{111,3}$	-0.064	–	–	$p^{\text{DR,gen}}_{111,3}$	-0.064	–	–	-0.064	–	–	-0.064	–	–
$p^{\text{DR,res}}_{112,3}$	-0.064	–	–	$p^{\text{DR,gen}}_{112,3}$	-0.064	–	–	-0.064	–	–	-0.064	–	–
$p^{\text{DR,res}}_{113,3}$	-0.128	–	–	$p^{\text{DR,gen}}_{113,3}$	-0.128	–	–	-0.128	–	–	-0.128	–	–
$p^{\text{DR,res}}_{114,3}$	-0.064	–	–	$p^{\text{DR,gen}}_{114,3}$	-0.064	–	–	-0.064	–	–	-0.064	–	–
$p^{\text{DR,res}}_{77,4}$	–	-0.080	–	$p^{\text{DR,gen}}_{77,4}$	–	0.000	–	–	0.000	–	–	-0.080	–
$p^{\text{DR,res}}_{79,4}$	-0.050	–	–	$p^{\text{DR,gen}}_{79,4}$	-0.050	–	–	-0.050	–	–	0.000	–	–
$p^{\text{DR,res}}_{80,4}$	–	-0.080	–	$p^{\text{DR,gen}}_{80,4}$	–	0.000	–	–	0.000	–	–	-0.080	–
$p^{\text{DR,res}}_{82,4}$	-0.080	–	–	$p^{\text{DR,gen}}_{82,4}$	-0.080	–	–	-0.080	–	–	-0.080	–	–
$p^{\text{DR,res}}_{85,4}$	–	–	-0.128	$p^{\text{DR,gen}}_{85,4}$	–	–	-0.064	–	–	-0.128	–	–	-0.128
				u_1		1			0			1	
				u_2		1			1			1	
				u_3		1			1			1	
				u_4		1			1			1	
				Load shed		none			55, 70			46, 47, 51-62, 64, 66-76, 79, 87-90, 94-98, 100-106, 109	

Table 3: Resource allocation results for case study 2. The first stage variables indicate the reserves purchased before the onset of the event (subject to expected event scenarios), while the second stage variables (three columns on the right) show how the purchased reserves are dispatched during the course of different event scenarios. The power values are per-unit quantities based on a 250kVA base power.

Table 4 summarizes these metrics for our problem instance. We observe that the stochastic solution and the "wait-and-see" solution are relatively close together, yielding to a relatively small EVPI. In contrast, the $\mathbb{E}$EV and the stochastic solution are significantly different, leading to a VSS of about 29% compared to the $\mathbb{E}$EV. That implies that the stochastic solution saves approx. 29% of the expected cost when using the deterministic approach (as described above).

We assumed that the "true" distribution of the line capacities, when a wildfire is approaching, is precisely given by the 10,000 samples. Because the resulting two-stage stochastic MIQCP is computationally intractable, we are forced to reduce the number of scenarios. Experimentally, we found that 100 scenarios is a good trade-off between solution quality and computational effort. Instead of randomly choosing 100 samples out of the 10,000 samples, we chose to utilize (optimal) scenario reduction. This is the reason why the values between the 100 and the 10,000 scenarios are so similar! When randomly choosing 100 scenarios, the results depend on our "luck." Since we are unable to solve our two-stage MIQCP model for the case of 10,000 scenarios to optimality, we selected an (optimal) first stage solution for the 100 scenario case and respond optimally by adjusting the recourse decision variables. Thus, the expected cost of \$296,311.25 is an upper bound on the optimal solution of the two-stage MIQCP with 10,000 scenarios. In contrast, the solutions for the "wait-and-see" model as well as for the $\mathbb{E}$EV are optimal.

We note that the results in Table 4 are sensitive to the load shedding penalty factor chosen. Nevertheless, the high value of the VSS relative to the stochastic solution is a strong indicator that a stochastic optimization framework is the method of choice when it comes to the optimal resilient power grid operation during wildfires.

	# of scenarios	
	100	10,000
Perfect information ("wait-and-see")	287,894.63	288,726.66
Stochastic solution ("here-and-now")	294,677.52	296,311.25♭
$\mathbb{E}$EV	418,841.49	420,412.48
Expected value of perfect information (EVPI)	6,782.89	$\leq$ 7,584.59
Value of the stochastic solution (VSS)	124,163.97	$\geq$ 124,101.23

Table 4: Quantifying the stochastic solution. ♭: We implemented the first stage decisions from the stochastic solution and solved the recourse decision to optimality for all 10,000 scenarios.

6. Conclusions

We studied a two-stage stochastic and nonlinear optimization problem which allows the utility operator to dispatch a power distribution network in the presence of a progressing wildfire, previously published in the literature. Our computational results show that the stochastic approach has a significant value over deterministic approaches. We find that this value comes from the asymmetry of the line capacity distribution: the mean capacity value is sufficient to yield a distribution network which can operate in the business-as-usual manner. As such, taking the expected value for the line capacity leads to the "no-disaster" solution. However, an extreme heat scenario results in very significant cost, if unhedged. The proposed stochastic optimization framework is able to pick up these phenomena and computes a solution which optimally balances the reserve cost vs. the expected costs resulting from a wildfire.

Appendix A. Case Study Data

Energy Resource	Node	Belongs to Microgrid	Capacity [kVA]	Cost of Reserve [c/kWh]	Cost of Energy [c/kWh]	Comments
DG	31	1	100	4	10	Phase c
DG	63	2	290	8	18	3-Phase
DG	65	2	440	8	18	3-Phase
DG	110	3	120	4	10	Phase a
DG	78	4	440	6	16	3-Phase
DR	31	1	27	4	8	Phase c
DR	32	1	27	5	8	Phase c
DR	33	1	34	5	8	Phase a
DR	63	2	34	4	8	Phase a
DR	65	2	210	8	14	3-Phase
DR	111	3	27	5	8	Phase a
DR	112	3	27	4	8	Phase a
DR	113	3	54	5	8	Phase a
DR	114	3	27	5	8	Phase a
DR	77	4	34	5.5	8	Phase b
DR	79	4	27	6	8	Phase a
DR	80	4	34	6	8	Phase b
DR	82	4	34	6	8	Phase a
DR	85	4	54	6	8	Phase c

Table A.5: DG and DR Load Data

References

[1] H. Rudnick, Natural Disasters – Their Impact on Electricity Supply, IEEE Power & Energy Magazine Mar/Apr. (2011) 22–24.

[2] K. Onoue, Y. Murakami, P. Sofronis, Japan's Energy Supply: Mid-to-Long-Term Scenario – A Proposal for a New Energy Supply System in the Aftermath of the March 11 Earthquake, International Journal of Hydrogen Energy 37 (2012) 8123–8132.

[3] S. K. Mohammadi, I. Hassanzadeh, R. Mathur, K. Patil, A New Fuzzy Decision-Making Procedure Applied to Emergency Electric Power Distribution Scheduling, Engineering Applications of Artificial Intelligence 13 (2000) 731–740.

[4] Y. Kumar, B. Das, J. Sharma, Multiobjective, Multiconstraint Service Restoration of Electric Power Distribution System with Priority Customers, IEEE Transactions on Power Delivery 23 (1) (2008) 261–270.

[5] D. Kleppinger, R. Broadwater, C. Scirbona, Generic Reconfiguration for Restoration, Electric Power Systems Research 80 (2010) 287–295.

[6] S. Dimitrijevic, N. Rajakovic, An Innovative Approach for Solving the Restoration Problem in Distribution Networks, Electric Power Systems Research 81 (2011) 1961–1972.

[7] M. Tsai, Y. Pan, Application of BDI-Based Intelligent Multi-Agent Systems for Distribution System Service Restoration Planning, European Transactions on Electric Power 21 (2011) 1783–1801.

[8] C. Nguyen, A. Flueck, Agent Based Restoration with Distributed Energy Storage Support in Smart Grids, IEEE Transactions on Smart Grid 3 (2) (2012) 1029–1038.

[9] F. Capitanescu, J. M. Ramos, P. Panciatici, D. Kirschen, A. M. Marcolini, L. Platbrood, L. Wehenkel, State-of-the-Art, Challenges, and Future

Trends in Security-Constrained Optimal Power Flow, Electric Power Systems Research 81 (8) (2011) 1731–1741.

[10] J. Condren, T. Gedra, Expected-Security-Cost Optimal Power Flow with Small Signal Stability Constraints, IEEE Transactions on Power Systems 21 (4) (2006) 1736–1743.

[11] B. Ansari, S. Mohagheghi, Optimal energy dispatch of the power distribution network during the course of a progressing wildfire, International Transactions on Electrical Energy Systems (2014) n/a–n/a`doi: 10.1002/etep.2043`.
URL `http://dx.doi.org/10.1002/etep.2043`

[12] B. Leblon, L. Bourgeau-Chavez, Wildfire, in: P. Bobrowsky (Ed.), Encyclopedia of Natural Hazards, Dordrecht, Netherlands: Springer, 2013, pp. 1102–1106.

[13] T. Seppa, Accurate Ampacity Determination: Temperature-Sag Model for Operational Real-Time Ratings, IEEE Transactions on Power Delivery 10 (3) (1995) 1460–1470.

[14] IEEE Standard 738-2006, IEEE Standard for Calculating the Current-Temperature of Bare Overhead Conductors.

[15] CIGRÉ WG 22.12, Thermal Behavior of Overhead Conductor, Electra (144).

[16] E. Koufakis, P. Tsarabaris, J. Katsanis, C. Karagiannopoulos, P. Bourkas, A Wildfire Model for the Estimation of the Temperature Rise of an Overhead Line Conductor, IEEE Transactions on Power Delivery 25 (2010) 1077–1082.

[17] J. Rossi, A. Simeoni, B. Moretti, V. Leroy-Cancellieri, An Analytical Model Based on Radiative Heating for the Determination of Safety Distances for Wildland Fires, Fire Safety Journal 46 (2011) 520–527.

[18] S. Frank, I. Steponavice, S. Rebennack, Optimal Power Flow: A Bibliographic Survey I – Formulations and Deterministic Methods, Energy Systems 3 (3) (2012) 221–258.

[19] S. Frank, I. Steponavice, S. Rebennack, Optimal Power Flow: A Bibliographic Survey II – Non-Deterministic and Hybrid Methods, Energy Systems 3 (3) (2012) 259–289.

[20] J. Kallrath, J. Wilson, Business Optimisation Using Mathematical Programming, MacMillian Press, 1997.

[21] Available at:. [link].
URL `http://ewh.ieee.org/soc/pes/dsacom/testfeeders/`

[22] F. Farret, M. Simões, Integration of Alternative Sources of Energy, Hoboken, NJ: John Wiley & Sons, Inc., 2006.

[23] G. Masters, Renewable and Efficient Electric Power Systems, Hoboken, NJ: John Wiley & Sons, Inc., 2004.

[24] H. Heitsch, W. Römisch, Scenario Reduction Algorithms in Stochastic Programming, Computational Optimization and Applications 24 (2003) 187–206.

[25] T. Westerlund, R. Pörn, Solving Pseudo-convex Mixed Integer Optimization Problems by Cutting Plane Techniques, Optimization and Engineering (2002) 253–280.

[26] R. Misener, C. Floudas, ANTIGONE: Algorithms for coNtinuous/Integer Global Optimization of Nonlinear Rquations, Journal of Global Optimization 59 (2014) 503–526.

[27] M. Tawarmalani, N. Sahinidis, A Polyhedral Branch-and-Cut Approach to Global Optimization, Mathematical Programming 103 (2) (2005) 225–249.

[28] J. Viswanathan, I. Grossmann, A combined Penalty Function and Outer Approximation Method for MINLP Optimization, Computers and Chemical Engineering 14 (1990) 769–782.

[29] R. Misener, C. Floudas, GloMIQO: Global Mixed-Integer Quadratic Optimizer, Journal of Global Optimization 57 (1) (2013) 3–50.

[30] R. Byrd, J. Gilbert, J. Nocedal, A Trust Region Method based on Interior Point Techniques for Nonlinear Programming, Mathematical Programming 89 (1) (2000) 149–185.

[31] Y. Lin, L. Schrage, The Global Solver in the LINDO API, Optimiation Methods and Software 24 (2009) 657–668.

[32] T. Achterberg, SCIP: Solving Constraint Integer Programs, Mathematical Programming Computations 1 (1) (2009) 1–41.